2 Structure

2.1 Coulomb interactions

While the information needed for reproduction of living systems is chiefly maintained in the sequence of macromolecules, any practical use of this information must rely on the physical forces that shape the molecules into functioning, sequence-dependent, structures. These forces and the resulting structures are the topic of the second segment of this course.

Since neither gravity, nor nuclear interactions, are particularly relevant to most organisms, the forces that shape the molecules of life are various manifestations of the electromagnetic interactions between electrons and nuclei. These include the strong covalent bonds (maintaining the primary connectivity of a molecule), the weaker hydrogen bonds (sensitive to orientations of the participating moieties), and the even weaker (and roughly direction independent) van der Waals forces. However, for these molecules to properly fold and function in the cell environment, their functionally relevant energy scales should be compared to the thermal energy k_BT at room temperature. Much higher energies freeze the corresponding degrees of freedom, while lower energies are irrelevant and ignored in comparison to the ubiquitous thermal fluctuations. Since entropic contributions to the free energy are also of the order of k_BT, entropic considerations play a major role at molecular and cellular levels. The following two sections emphasize the role of entropy in the context of ionic interactions and polymer conformations.

2.1.1 Charge dissociation in solution

Entropy is indeed the reason why many molecules (electrolytes) dissociate and ionize in solution. The opposing charges making up an ion clearly minimize the Coulomb energy by being in close proximity in a bound (molecular) state. The loss of this electrostatic energy in the dissociated (ionized) state is balanced by the gain in configurational entropy. We can quantify this by an approximate evaluation of the change in free energy upon dissociation, as

$$\Delta F = \Delta E - T\Delta S = -\mathcal{E}_b + k_BT \log\left(\frac{V}{Nv_0}\right). \tag{2.1}$$

Here, $\mathcal{E}_b$ is the binding energy, T is the temperature, k_B is the Boltzmann constant, and v_0 is some characteristic volume. The gain in entropy is estimated from the number of positions available for each of N particles in the volume V. (A systematic evaluation of the partition function reproduces the above result with $v_0 = \lambda^3$, where λ is the "thermal wavelength.") Setting the free energy change to zero, gives the equilibrium concentration

$$c = \frac{N}{V} = \frac{1}{\lambda^3} e^{-\beta\mathcal{E}_b}. \tag{2.2}$$

The electrostaic contribution to the binding energy of opposite charges, $\mathcal{E}_c$, can be estimated from Coulomb's law, as

$$\mathcal{E}_c = \frac{q_1 q_2}{\epsilon r} = -\frac{e^2 z^2}{\epsilon r}, \tag{2.3}$$

where ϵ is the dielectric constant of medium- water in cases of interest to us, z is the valence, and e is the electron charge. The physically significant quantity is the ratio of this energy to the thermal energy k_BT, which can be expressed as

$$-\beta\mathcal{E}_c = \frac{\beta e^2 z^2}{\epsilon r} = z^2 \frac{l_B}{r}, \tag{2.4}$$

where we have defined the *Bjerrum length*

$$l_B = \frac{e^2}{\epsilon k_B T}. \tag{2.5}$$

For water, $\epsilon \approx 81$, and the Bjerrum length is about 7.1 Å at room temperature. Very roughly, we may surmise that at separations larger than l_B, the Coulomb interaction between unit charges in water is insignificant compared to the thermal energy.

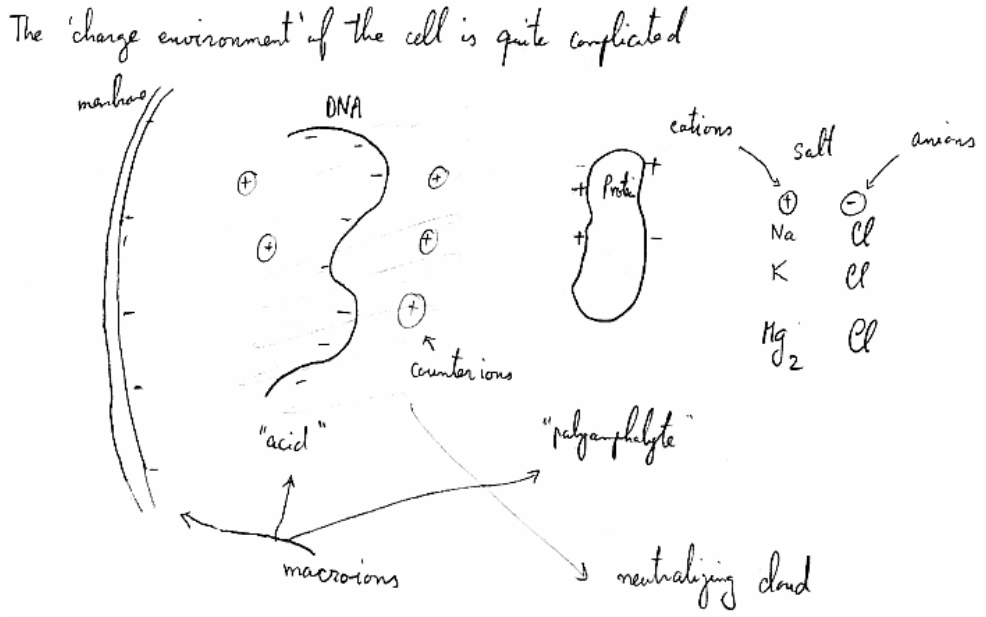

Figure 1: The charge environment of a cell.

We can also think of dissociation as the chemical reaction

$$CA \rightleftharpoons C_+ + A_- \,. \tag{2.6}$$

(The dissociated positive charge is called a *cation*, the negative one an *anion*.) The *equilibrium constant* of the reaction, expressed in terms of the concentrations of the different components as

$$K_{eq.} \equiv \frac{[C_+][A_-]}{[CA]} \propto e^{-\beta\mathcal{E}_b}, \tag{2.7}$$

is a measure of the ease with which ionization occurs. For strong electrolytes, such as Na^+Cl^- (salt), Na^+OH^- (base) and H^+Cl^- (acid), which dissociate almost totally, the net binding energy is small. Weaker electrolytes are more strongly bound and dissociate less readily. Water itself can dissociate into H^+ and OH^- ions, but at room temperature this process only produces about 10^{-7} hydrogen ions per mole.

Biological molecules also dissociate, and the 'charge environment' of a cell is quite complicated. The lipids forming the cell membrane become negatively charged upon dissociation, as does DNA. The latter is an acid that releases H^+ ions, leaving behind a negatively charged backbone. Proteins can also release H^+ ions, but some of the amino-acid side groups are actually *basic,* releasing OH^-. A molecule of this sort, which can develop regions both of positive and of negative charge upon dissociation, is called a *polyampholyte.* Molecules like the DNA backbone, which carry a uniform charge, are known as *polyelectrolytes.* Generically, both types of macromolecules are referred to as *macroions,* and the small charged particles they give up into the cytoplasm are called *counterions.* The electrostatic interactions between the macromolecules are very important for their biological function– the repulsive forces prevent aggregation, while attractions are important for docking and recognition. However, calculating these interactions in the environment of the moving counterions is not an easy task.

2.1.2 The Poisson–Boltzmann Equation

We know that proteins bind to one another, and that some proteins bind to DNA. In principle, an effective Coulomb interaction between such macroions can be obtained by holding them at fixed separation (and orientation); a constrained partition function is then evaluated by integrating over all the other degrees of freedom, e.g. the positions of the mobile counterions, as

$$e^{-\beta F(\text{macroions})} = Z_{\text{res.}} = \int \prod_i d^3 r_i \, e^{-\beta \mathcal{H}_c}. \tag{2.8}$$

In addition to steric constraints (the excluded volume around each atom), the Hamiltonian $\mathcal{H}_c$ includes the direct Coulomb interactions between the macroions, their interactions with the counterions, as well as the interactions amongst counterions. The restricted partition function is too hard to compute directly, and we shall instead resort to a "mean-field" approximation in which each counterion is assumed to experience an effective potential $\phi(\vec{r})$ due to the macroion, as well as all the other counterions. The effective potential is then computed self-consistently.

In this approximation, the position-dependent density of counterion species α (with valence z_α) adjusts to the potential through the Boltzmann weight, as

$$n_\alpha(\vec{r}) = \bar{n}_\alpha \exp\left[-\beta \phi(\vec{r}) z_\alpha e\right]. \tag{2.9}$$

Note that $\bar{n}_\alpha$ is in general not the particle density, but an overall parameter that needs to be adjusted so that when the density is integrated over $\vec{r}$ the correct number of counterions is

obtained. The potential $\phi(\vec{r})$ is in turn determined by the charge distribution, and satisfies the Poisson equation,

$$\nabla^2\phi = -\frac{4\pi}{\epsilon}\rho(\vec{r}). \tag{2.10}$$

The charge density at each point has a contribution from the macroions, and from the (fluctuation averaged) counterion density, and thus

$$\rho(\vec{r}) = \rho_{\rm macroions}(\vec{r}) + \sum_\alpha z_\alpha e\bar{n}_\alpha e^{-\beta\phi z_\alpha e}. \tag{2.11}$$

Self-consistency then leads to the *Poisson-Boltzmann Equation*

$$\nabla^2\phi = -\frac{4\pi}{\epsilon}\left[\rho_{\rm macroions}(\vec{r}) + \sum_\alpha z_\alpha e\bar{n}_\alpha e^{-\beta\phi z_\alpha e}\right], \tag{2.12}$$

This equation, while a drastic simplification of the original problem, is commonly used for study of ionic solutions. It is a *non-linear* partial differential equation, and exact solutions are available only for a few simple geometries. It does have the virtue of being at least numerically solvable.

2.1.3 Debye screening by salt ions

We expect physically that counterions will accumulate near regions of opposite charge to lower the electrostatic energy. As a result a charged macroion will be surrounded by a cloud of counterions, shielding and reducing its net charge. This effect is easily captured in a linearized version of Eq. (2.12). Expanding the Boltzmann weight in powers of ϕ is actually a quite good strategy when the Coulomb interaction between macroions is *screened* by a high concentration of salt ions. The first step is to linearize the exponential such that the local counterion charge density is

$$\rho_c(\vec{r}) = \sum_\alpha ez_\alpha\bar{n}_\alpha e^{-\beta z_\alpha e\phi} \approx \sum_\alpha ez_\alpha\bar{n}_\alpha\left[1-\beta z_\alpha e\phi+\cdots\right]. \tag{2.13}$$

We note that at this order the local variations in counterion charge density and potential are simply proportional. Integrating the linearized equation for $n_\alpha(\vec{r})$, we find the total number $N_\alpha = \bar{n}_\alpha V\left[1-\beta ez_\alpha\bar{\phi}\right]$. The value of the potential is in fact arbitrary up to a constant (which then adjust $\bar{n}$. Thus without loss of generality we can set $\bar{\phi}=0$, in which case we can replace $\bar{n}_\alpha$ with the overall density $n_\alpha = N/V$. The mobile ions are a mixture of cations and anions from the dissociation of salt molecules in the solution, and counterions (typical H^+ and OH^{-1}) from dissociation of the macroions. The contribution of salt ions to the first term in Eq. (2.13) vanishes due to their overall charge neutrality, and neglecting the much smaller contribution from counterions released by the macroions (at high salt concentrations), we find

$$\boxed{\nabla^2\phi = -\frac{4\pi}{\epsilon}\rho_{\rm macroions}(\vec{r}) + \frac{\phi}{\lambda^2},} \tag{2.14}$$

where

$$\boxed{\lambda^{-2} = \sum_\alpha \frac{4\pi}{\epsilon}\beta e^2 z_\alpha^2 n_\alpha = 4\pi l_B \sum_\alpha z_\alpha^2 n_\alpha.} \tag{2.15}$$

This is the *Debye-Hückel* equation, and the parameter λ is the Debye *screening length.* In a typical biological environment λ is around 1nm.

For the case of a single point charge $Q = ze$, with

$$\rho_{\text{macroion}}(\vec{r}) = ze\delta^3(r), \tag{2.16}$$

the solution is the exponentially damped version of the Coulomb potential

$$\phi(\vec{r}) = k_B T \frac{z l_B}{|\vec{r}|} e^{-\frac{|\vec{r}|}{\lambda}}. \tag{2.17}$$

Since Eq. (2.14) is linear, its solution for a general distribution of charges is obtained by simple superposition, leading to the interaction energy

$$\beta E_{\text{interactions}}(\text{macroions}) = l_B \sum_{m<n} \frac{z_m z_n}{|\vec{r}_{mn}|} e^{-\frac{|\vec{r}_{mn}|}{\lambda}}. \tag{2.18}$$

2.1.4 Dissociation from a plate

The Debye-Hückel approximation is not applicable at low salt density. For example, consider the simple geometry of a flat plate, reminiscent of a membrane, with no salt in the ambient water solution. Upon dissociation the membrane is negatively charged; its charge density denoted by $\sigma = -e/d^2$ (i.e. the negative charges are on average a distance d apart, and their discreteness is ignored). The neutralizing counterions, of charge $+e$ are present in the solution on both sides of the membrane. Due to translational symmetry, the average charge density (and potential) only depend on the separation from the plate, indicated by the coordinate y, and full Poisson–Boltzmann Eq. (2.12) now reads

$$\frac{d^2\phi}{dy^2} = -\frac{4\pi}{\epsilon} e\bar{n} e^{-\beta e\phi(y)}. \tag{2.19}$$

The following trick allows us to guess the solution to Eq. (2.19). We first make a transformation to

$$W(y) = e^{\beta e\phi/2} \quad \Longrightarrow \quad \phi = \frac{2}{\beta e}\log W, \tag{2.20}$$

such that

$$\phi' = \frac{2}{\beta e}\frac{W'}{W}, \quad \text{and} \quad \phi'' = \frac{2}{\beta e}\cdot\frac{W''W - W'^2}{W^2}.$$

Multiplying both sides by W^2, Eq. (2.19) can be recast as

$$\frac{2}{\beta e}\left(W''W - W'^2\right) = -\frac{4\pi}{\epsilon} e\bar{n}\,. \tag{2.21}$$

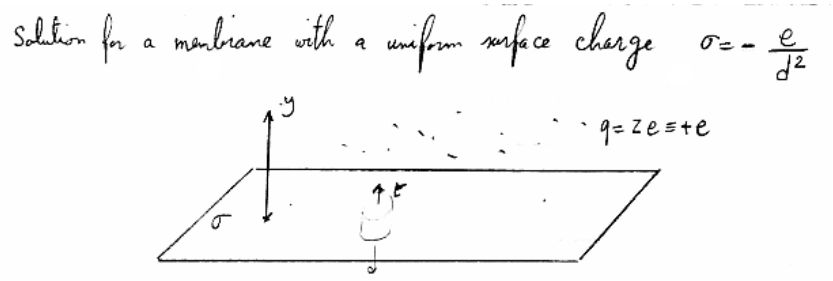

Figure 2: Membrane with a uniform surface charge.

While still non-linear, it is easy to see that a linear function of y satisfies the above equation, and we set

$$W(y) = 1 + \frac{y}{y_0}\,, \tag{2.22}$$

where, without loss of generality, we have set $\phi(y \to 0) = 0$, such that $W(0) = 1$, and $y_0^{-2} = 2\pi\beta e^2 \bar{n}/\epsilon$. Note, however, that $\bar{n}$ is simply a parameter that needs to be set by the requirement of charge neutrality. It is easier to trade in this parameter for y_0 and constrain the latter. The electrostatic potential thus has the form

$$\phi(y) = \frac{2}{\beta e} \log\left[1 + \frac{y}{y_0}\right]. \tag{2.23}$$

The undetermined length, y_0, clearly sets the scale at which the counterion density changes significantly. It can be determined by examining the limit $y \ll y_0$, for which Eq. (2.23) becomes

$$\phi(y) \approx \frac{2}{\beta e}\frac{y}{y_0}. \tag{2.24}$$

Indeed, at distances close enough to the surface that screening is unimportant, we expect the electric field to be (e.g. by appealing to a Gaussian pillbox)

$$E = \frac{2\pi\sigma}{\epsilon},$$

and a corresponding potential

$$\phi = -\frac{2\pi\sigma}{\epsilon} y\,. \tag{2.25}$$

Comparing this result with Eq. (2.24) indicates that

$$y_0 = \frac{\epsilon}{e\sigma\pi\beta} = \frac{\epsilon}{\beta e^2}\frac{d^2}{\pi} = \frac{d^2}{\pi l_B}\,. \tag{2.26}$$

This characteristic scale, known as the *Guoy-Chapman length*, determines the thickness of the so-called"diffusive boundary layer" of ions that shields a charged membrane.

Retracing the steps of algebra, it is easy to check that

$$\bar{n} = \frac{\pi}{2}\frac{l_B}{d^4}\,,$$

and

$$n(y) = \frac{\bar{n}}{W^2} = \frac{\pi}{2}\frac{l_B}{d^4}\left(1+\frac{y}{y_0}\right)^{-2}\,. \tag{2.27}$$

At large separations, $y \gg y_0$, from the plate, the counterion density falls off as $(2\pi l_B y^2)^{-1}$. The corresponding potential behaves as $\phi(y) \approx 2\ln(y)/(\beta e)$, very different from the linear potential in vacuum, and also quite distinct from an exponential decay that may have been surmised based on Debye-Huckel screening. Clearly this type of screening will lead to a quite different interaction between charged plates, a question that will be taken up in the next problem set. In connection to that, we note that Eq. (2.21) also admits solutions of the form $\cos(y/y_1+\theta)$ with parameters y_1 and θ that can be adjusted to conform to the boundary conditions corresponding to parallel charged plates.

While the solutions to the Poisson-Boltzmann equation are interesting and informative, they do not capture the entire physics of the problem. Fluctuations in charge density can be important in lowering the free energy. Indeed at high temperatures the correlated fluctuations around two similarly charged macroions further reduce the repulsion through a dipole-dipole interaction reminiscent of the van der Waals force. If strong enough, these fluctuations can entirely reverse the sign of the force, leading to an attractive interaction between like-charged macroions. Such phenomena, not captured by the Poisson-Boltzmann equation, have received considerable attention in recent years.

2.2 Fluctuating Polymers

The basic molecules of life (DNA, RNA, proteins, $\cdots$) are *hetero-polymers*, formed by the covalent bonding of a sequence of elementary units (nucleic acids, amino-acids) in long chains. A *homo-polymer*, as in many synthetic organic molecules, is constructed by joining $N \gg 1$ copies of the same monomer. A simple example is *polyethylene*,

$$|-CH_2-|_N \equiv \qquad \cdots - CH_2 - CH_2 - CH_2 - \cdots \qquad .$$

The *degree of polymerization*, i.e. the the number of repeated units, can be quite large, ranging from a few hundred for proteins, $10^4 - 10^5$ for polyethelene, to as big as 10^9 for some DNA. Typically the covalent bonds holding the polymer together are strong and cannot be broken at room temperature. There can, however, be flexibility in aligning/bending successive monomers, resulting in a large number of configurational degrees of freedom for polymers, indicating that a statistical description of the problem is fruitful. Such a statistical perspective is useful for describing general properties common to both synthetic and natural polymers. For example, at very high (not necessarily physiological) temperatures all polymers will be in a swollen (denatured) state to take maximum advantage of entropy. The heterogeneity of the sequence is irrelevant in such a phase, and we shall thus initially focus on the fluctuations of a homo-polymer.

2.2.1 Rotational isomers

Successive carbon–carbon bonds in the chain can be in different relative orientations, called *rotational isomers*. In polyethelene, the low energy *trans* conformation leads to a parallel alignment of bonds. There are two higher energy *gauche* states which form an angle of $2\pi/3$ between successive bonds. Assuming an energy difference Δ between the trans and gauche states, at a temperature T, the probabilities of these outcomes satisfy the Boltzmann weight

$$\frac{\text{prob.}(g)}{\text{prob.}(t)} = 2e^{-\beta\Delta}, \qquad \text{with} \qquad \beta = \frac{1}{k_B T}.$$

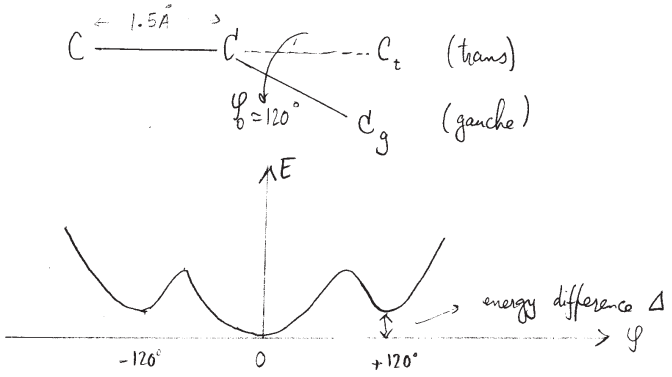

Figure 3: Trans–gauche configurations of a polymeric bond.

For $(CH_2)^N$, Δ is quite small (roughly 500 cal/mole or $1/3k_BT$), and the polymer is very flexible at room temperature. For other polymers $\Delta > k_BT$, and gauche states with probability

$$p(g_+) = p(g_-) = \frac{e^{-\beta\Delta}}{1 + 2e^{-\beta\Delta}},$$

are relatively rare. A typical configuration then consists of long straight segments with few bends. The probability of a straight segment of n monomers is $p_t^n(1-p_t)$, where $p_t = 1-2p(g)$ is the probability of a trans bond. The average length of straight segments is thus $\langle n \rangle a$, where a is the bond length (monomer size), and

$$\langle n \rangle = -\frac{1}{\ln p_t} = \left(\ln\left[1 + 2e^{-\beta\Delta}\right]\right)^{-1}. \tag{2.28}$$

The typical size of these linear segments is proportional to the *persistence* of the polymer. The *persistence length* characterizes the decay of orientational correlations along the chain. In the above simplified model, let us denote the orientation of the bonds by the set of vectors $\{\vec{t}_1, \vec{t}_2, \cdots, \vec{t}_N\}$, with $\vec{t}_j \cdot \vec{t}_j = a^2$. Assuming that the (two) gauche states produce a relative bond angle ϕ, we have

$$\left\langle \vec{t}_1 \cdot \vec{t}_2 \right\rangle = a^2 \frac{1 + 2\cos\phi e^{-\beta\Delta}}{1 + 2e^{-\beta\Delta}} \approx a^2 \exp\left[-2(1-\cos\phi)e^{-\beta\Delta}\right],$$

where the last expression is valid in the limit of $\beta\Delta \gg 1$ where a gauche state is very unlikely. In the same approximation, the correlation between bonds that are further apart is given by

$$\left\langle \vec{t}_1 \cdot \vec{t}_{n+1} \right\rangle \approx a^2 \frac{1 + 2n\cos\phi e^{-\beta\Delta} + \mathcal{O}(e^{-2\beta\Delta})}{1 + 2ne^{-\beta\Delta} + \mathcal{O}(e^{-2\beta\Delta})} \approx a^2 \exp\left[-2n(1-\cos\phi)e^{-\beta\Delta}\right],$$

where we have included only configurations with one gauche bond. The orientation correlations decay exponentially as $e^{-\ell/\xi_p}$, where $\ell = na$ is the counter-length along the polymer, and the persistence length ξ_p is given by

$$\xi_p \approx \frac{ae^{\beta\Delta}}{2(1-\cos\phi)}. \tag{2.29}$$

2.2.2 Worm-like chain

For a rigid polymer such as double-stranded DNA a kink causing a finite rotational angle is energetically costly and does not occur. The loss of angular correlations at long distances then occurs from the accumulation of small changes from one monomer to the next. If we indicate as before a polymer configuration by the set of vectors $\{\vec{u}_i \equiv \vec{t}_i/a\}$, we can approximate the energy of a nearly straight configuration by

$$\mathcal{H} = -J \sum_{i=1}^{N-1} \vec{u}_i \cdot \vec{u}_{i+1}\,. \tag{2.30}$$

Since in a typical configuration $\vec{t}$ changes slowly, it is useful to go over to a *continuum limit* in

Figure 4: The wormlike chain.

which the discrete monomer index i is replaced by the continuous *arc-length* $s \in [0, L = Na]$. Using $(\vec{u}_i - \vec{u}_{i+1})^2 = 2 - 2\vec{u}_i \cdot \vec{u}_{i+1}$, and replacing $\sum_{i=1}^{N-1}$ with $\int_o^L ds/a$, we obtain

$$\mathcal{H} \approx -JN + \frac{\kappa}{2}\int_0^L ds \left(\frac{d\vec{t}}{ds}\right)^2, \tag{2.31}$$

where $\kappa = Ja$ is the coefficient of *bending rigidity*. (Note that $|d\vec{u}/ds| = 1/R(s)$, where $R(s)$ is the local radius of curvature.)

Ignoring the initial energy of the "ground state" configuration, it is common to write the energy in dimensionless form as

$$\beta\mathcal{H} = -\frac{\xi_p}{2}\int_0^L ds \left(\frac{d\vec{u}}{ds}\right)^2, \tag{2.32}$$

with $\beta\kappa = \xi_p$. We have anticipated that the bending rigidity is related to the persistence length. In fact, it can be shown (e.g. by using transfer matrices) that for the discrete model of Eq. (2.30)

$$\langle \vec{u}_m \cdot \vec{u}_n \rangle \approx \left(\coth(\beta J) - \frac{1}{\beta J} \right)^{|m-n|} \quad \text{for} \quad |m-n| \gg 1, \tag{2.33}$$

and thus in the continuum limit

$$\langle \vec{t}(s) \cdot \vec{t}(s+\ell) \rangle \approx a^2 e^{-\ell/\xi_p}, \tag{2.34}$$

with $\xi_p \approx \beta\kappa$ for $\beta J \gg 1$. This, so called *worm-like chain* model is frequently invoked as a description of double-stranded DNA, where ξ_p is in the range of 50-100nm.

2.2.3 Entropic elasticity

The flexibility of long polymers arises from the statistical fluctuations of segments larger than the persistence length. The important parameter that governs the number of configurations is thus not the degree of polymerization N, but the number of unconstrained degrees of freedom, or the *Kuhn* length $N_K \approx Na/(2\xi_p)$. To see this explicitly, let us consider the *end to end separation* of the polymer, given by

$$\vec{R} = \vec{t}_1 + \vec{t}_2 + \cdots + \vec{t}_N = \sum_{i=1}^{N} \vec{t}_i \, .$$

Because of rotational symmetry (there is no cost for rotating the entire polymer), $\langle \vec{R} \rangle = 0$, and its variance is given by

$$\langle R^2 \rangle = \sum_{i,j=1}^{N} \langle \vec{t}_i \cdot \vec{t}_j \rangle = Na^2 + 2 \sum_{i<j} \langle \vec{t}_i \cdot \vec{t}_j \rangle \, . \tag{2.35}$$

We shall assume that the orientational correlations decay as a simple exponential (this is only asymptotically correct), i.e.

$$\langle \vec{t}_i \cdot \vec{t}_j \rangle = a^2 e^{-a|i-j|/\xi_p} \, . \tag{2.36}$$

As the correlation function is the same for every pair of points separated by a distance k, and as there are $(N-k)$ such pairs along the chain

$$\langle R^2 \rangle = Na^2 + 2a^2 \sum_{k=1}^{N} (N-k) e^{-ak/\xi_p} \, . \tag{2.37}$$

The above geometric series are easily summed, and for $N \gg 1$ (where only the term proportional to N is significant), we obtain

$$\langle R^2 \rangle = Na^2 \left(1 + \frac{2e^{-a/\xi_p}}{1 - e^{-a/\xi_p}} \right) = Na^2 \coth\left(\frac{a}{2\xi_p} \right) \tag{2.38}$$

$$\approx 2Na\xi_p = (2\xi_p)^2 \left(\frac{Na}{2\xi_p} \right) \, . \tag{2.39}$$

The approximations in the second line rely on $\xi_p \gg a$. The very last expression indicates that the behavior of the variance is the same as that of $N_K \equiv (Na/2\xi_p)$ independent rods of length $2\xi_p$, i.e. the same variance is obtained for a collection of N_K *freely–jointed rods*, each of length $2\xi_p$. Indeed the correlations between these Kuhn segments is sufficiently small that in the limit of $N_K \gg 1$, we expect the *Central Limit Theorem* to hold, leading to the probability distribution function

$$p(\vec{R}) = \exp\left[-\frac{3R^2}{2\langle R^2\rangle}\right]\left(\frac{2\pi\langle R^2\rangle}{3}\right)^{3/2} = \exp\left[-\frac{3R^2}{4Na\xi_p}\right]\frac{1}{(4\pi Na\xi_p/3)^{3/2}}\,. \tag{2.40}$$

The final probability distribution is identical to the Boltzmann weight of a Hookian spring of strength $J_{polymer}$ connecting the end points of the polymer, and the result of entropic fluctuations can be interpreted as conferring an elastic bond between the ends of the polymer with spring coefficient

$$J_{polymer} = \frac{3k_BT}{\langle R^2\rangle} = \frac{3k_BT}{2Na\xi_p}. \tag{2.41}$$

2.3 Interacting Polymers

The polymeric properties discussed so far arose from the flexibility of the covalent bonds that join adjacent monomers. There are also interactions between any other pairs (triplets, etc.) of monomers which depend on their spatial vicinity and that favor certain spatial configurations. Indeed, it is such interactions, typically due to hydrogen bonds, that enable proteins to fold and assume specific shapes. There are competing effects due to thermal fluctuations and competition with solvent interactions.

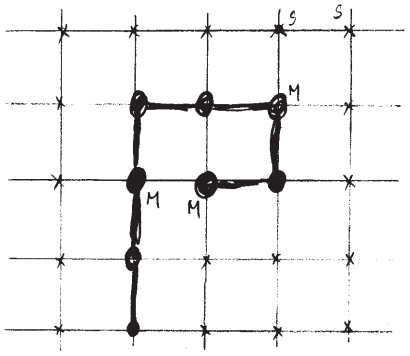

Figure 5: A self-avoiding walk on the square lattice.

Some of the ingredients of polymer interactions in a solvent is present in the very simple model of chain configurations on a (say square) lattice. The set of *random walks* on the square lattice that do not step back to the previous site grows with the number of steps N as 3^N. One simple consequence of interactions is that it is physically impossible to visit a previously occupied site. The steric constraint of *excluded volume* prunes the random walks

to a smaller subset of so-called *self-avoiding walks*. The number of self-avoiding walks also grows exponentially as g^N with $g < 3$ ($g \approx 2.64$).

A simple way to incorporate interactions on a lattice is to count the number of (non-polymeric) nearest-neighbor pairs, and assign energy

$$E = \epsilon_{mm} N_{mm} + \epsilon_{ms} N_{ms} + \epsilon_{ss} N_{ss},$$

where mm, ms, and ss stand for monomer-monomer, monomer-solvent, and solvent-solvent pairs respectively, with N_{pair} and ϵ_{pair} indicating the corresponding number and bond-energies. As two initially separate monomers are brought into contact, two ms bonds are replaced by one mm bond and one ss bond, leading to a change in energy of $\delta\epsilon = \epsilon_{mm} + \epsilon_{ss} - 2\epsilon_{ms}$. The preference of the monomers to aggregate in solvent is thus captured by the dimensionless *"Flory–Huggins"* parameter

$$\chi \equiv -\frac{\beta}{2}\delta\epsilon = \beta\left(\epsilon_{ms} - \frac{\epsilon_{mm} + \epsilon_{ss}}{2}\right). \tag{2.42}$$

A negative χ leads to separation of monomers, while a positive χ encourages their aggregation.

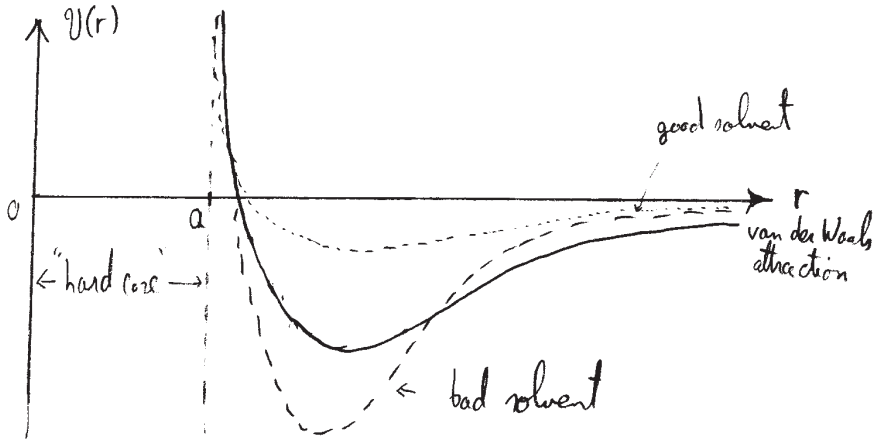

Figure 6: Effective interaction between monomers in a solvent.

In a more realistic model, the interactions between molecules vary continuously as a function of their relative separation and orientation in space. The dependence on orientation is particularly relevant to hydrogen bonding, while the van der Waals attraction mainly depends on the separation. Just as in Eq. (2.8), an effective potential $\mathcal{V}(r)$ between monomers is in principle obtained by integrating over all positions (and orientations) of the solvent particles. In the usual case where the monomers are larger than the solvent molecules, the effective potential is attractive at large distances and has a hard repulsive core at short distances. For a good solvent the potential is weak, while a strong attractive potential favors aggregation of monomers in a bad solvent. The quality of solvent also changes as a function of temprature due to entropic contributions of its constituents. The larger entropy of solvent molecules typically improves the quality of a solvent at higher temperatures.

2.3.1 Mean-field estimate of the partition function

To calculate the properties of a polymer in solvent– e.g. to determine if it is in its native form or a denatured state at some temperature– we need to compute the free energy of the molecule and it environment. Computation of the partition function is a hard task, even for the highly simplified models we have introduced so far. We shall instead rely upon an approximate expression obtained in a mean-field/variational treatment. Let us assume that the most likely configurations of an interacting homopolymer have a typical size R. The partition of N monomers confined to a sphere of radius R is then estimated as

$$\begin{aligned} Z(N,R) &\approx g^N \times \frac{\exp\left(-\frac{3R^2}{4Na\xi_p}\right)}{(4\pi Na\xi_p/3)^{3/2}} \\ &\times \left\{1\cdot\left[1-\left(\frac{a}{R}\right)^3\right]\cdot\left[1-2\left(\frac{a}{R}\right)^3\right]\cdots\left[1-(N-1)\left(\frac{a}{R}\right)^3\right]\right\}\times e^{-\beta E_{att.}}\,. \end{aligned} \tag{2.43}$$

The first line in Eq. (2.44) pertains to the entropy of the polymer, the first term encodes the exponential growth in the number of configurations of an unconstrained polymer– the precise value of g is in fact irrelevant to the considerations that follow. The second term approximates the reduction in the number of configurations when the polymer is constrained to a size R. The effect of this reduction is included as a Hookian spring, motivated by the result in Eq. (2.40) for the end-to-end probability of a non-interacting polymer.

The second line in Eq. (2.44) approximates the effect of interactions and is broken into two parts. The first part encodes the reduction in phase space due to excluded volume constraints: the first monomer is unconstrained, the volume available to the second is reduced by the fraction $(a/R)^3$ due to the volume excluded by the first, and so on. The reductions due to the excluded volume make a contribution to the free energy proportional to

$$\begin{aligned} \delta \ln Z_{EV} = \sum_{i=1}^{N-1} \ln\left[1-i\left(\frac{a}{R}\right)^3\right] &\approx -\left(\frac{a}{R}\right)^3\sum i - \frac{1}{2}\left(\frac{a}{R}\right)^6\sum i^2 + \cdots \\ &\approx -\frac{N^2}{2}\left(\frac{a}{R}\right)^3 - \frac{N^3}{6}\left(\frac{a}{R}\right)^6 - \cdots\,. \end{aligned} \tag{2.44}$$

The attractive part of the interaction, for homopolymers, is given by

$$E_{att.} = \frac{1}{2}\sum_{i\neq j}\mathcal{V}(\vec{r}_i-\vec{r}_j) = \frac{1}{2}\int d^3\vec{r}d^3\vec{r}'n(\vec{r})n(\vec{r}')\mathcal{V}(\vec{r}-\vec{r}')\,. \tag{2.45}$$

Assuming a uniform mean-density, $n(\vec{r}) = n = N/V = N/(4\pi R^3/3)$, leads to

$$E_{att.} = \frac{n^2}{2}V\int_a d^3\vec{r}\mathcal{V}(\vec{r})\,, \tag{2.46}$$

where we have integrated over the center of mass of the pair to get the volume V, and ignored any contributions from the surface. In the spirit of Flory-Huggins, we introduce a

dimensionless parameter χ, via

$$\int_a d^3\vec{r}\mathcal{V}(\vec{r}) \equiv \left(-\frac{4\pi}{3}a^3\right) k_B T(2\chi)\,, \tag{2.47}$$

to capture of the net effect of attractions, and such that

$$-\beta E_{att.} = N^2 \left(\frac{a}{R}\right)^3 \chi\,. \tag{2.48}$$

The resulting free energy, with R as a variational parameter,

$$\begin{aligned} \ln Z(N,R) &= N\ln g - \frac{3}{2}\ln\left[\frac{4\pi N a\xi_p}{3}\right] - \frac{3R^2}{4Na\xi_p} \\ &- \frac{N^2}{2}\left(\frac{a}{R}\right)^3 - \frac{N^3}{6}\left(\frac{a}{R}\right)^6 - \cdots + \chi N^2\left(\frac{a}{R}\right)^3\,, \end{aligned} \tag{2.49}$$

will next be used to explore the phases of the interacting homopolymer.

2.3.2 Swollen (coil) polymers in good solvents

Most of the terms in the trial free energy of Eq. (2.49) have definite sign. The exception is the term proportional to $N^2(a/R)^3$ which has opposing contributions from the repulsive and attractive parts of the potential, and is proportional to $(\chi - 1/2)$. The sign of this term determines whether attraction or repulsion is the dominant effect, leading to two different phases. For $\chi < 1/2$ repulsion is more important favoring large R and swollen polymers. This tendency is opposed by the reduction of entropy at larger R. Indeed, one can self-consistently check that all other terms are less important in this limit, such that

$$\ln Z(N,R) = \text{constant} - \frac{3R^2}{4Na\xi_p} - \frac{1-2\chi}{2}N^2\left(\frac{a}{R}\right)^3 + \text{higher order terms.} \tag{2.50}$$

Extremizing the above expression leads to

$$\frac{\partial \ln Z}{\partial R} = -\frac{3R}{2Na\xi_p} + \frac{3(1-2\chi)}{2}N^2\left(\frac{a^3}{R^4}\right) \;\Rightarrow\; \overline{R}^5 = (1-2\chi)a^4\xi_p N^3\,,$$

$$\overline{R} = (1-2\chi)^{1/5}(a^4\xi_p)^{1/5}N^{3/5}\,. \tag{2.51}$$

In the absence of interactions, the typical size of the polymer grows as $\sqrt{a\xi_p N}$, Eq. (2.39). An interesting consequence of repulsion due to excluded volume is that the scaling of size is changed to $R \propto N^\nu$, with an exponent $\nu > 1/2$. The variational treatment leading to Eq. (2.51) thus predicts the so-called *Flory exponent* of $\nu = 3/5$.

Going beyond the mean-field variational treatment is not trivial, and one of the triumphs of renormalization group theory is to estimate the exact value of $\nu = 0.591\ldots$, remarkably close to the Flory approximation of 3/5. While not directly relevant to real polymers, it is

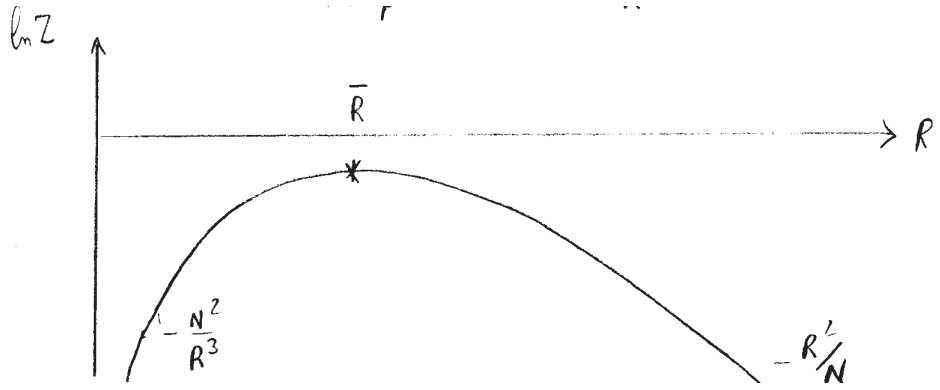

Figure 7: Variational free energy for a swollen polymer.

possible to inquire about the exponent ν for self-avoding walks in d-spatial dimensions– e.g., for polymers confined to a $d = 2$ dimensional surface. Ignoring the attractive part of the interaction, but incorporating the repulsive cores, generalizes Eq. (2.52) to

$$\ln Z(N, R) = \text{constant} - \frac{dR^2}{4Na\xi_p} - \frac{N^2}{2}\left(\frac{a}{R}\right)^d . \tag{2.52}$$

Extremization now gives

$$\frac{\partial \ln Z}{\partial R} = -\frac{dR}{2Na\xi_p} + \frac{d}{2}N^2\left(\frac{a^d}{R^{d+1}}\right) \Rightarrow \overline{R} = \left(a^{d+1}\xi_p\right)^{\frac{1}{d+2}} N^{\frac{3}{d+2}} ,$$

i.e. a generalized Flory exponent of

$$\nu_F(d) = \frac{3}{d+2} . \tag{2.53}$$

The predicted values of $\nu = 1,\ 3/4,\ 1/2$ in $d = 1,\ 2,\ 4$ are in fact exact. Above four dimensions the excluded volume constraint is irrelevant and ν remains fixed at $1/2$.

2.3.3 Compact (globular) polymers in bad solvents

On lowering temperature $\chi(T)$ typically becomes larger, and the coefficient $(1 - 2\chi)$ in Eq. (2.52) changes sign at the so-called θ-point ($\chi(\theta) = 1/2$). At temperatures $T < \theta$ the attractive component of the interaction is more important, leading to compact (globular) shapes with a finite number density $\rho = N(a/R)^3$. The leading terms in the expansion of the variational free energy can now be recast as

$$-\frac{\ln Z(\rho)}{N} = -\ln g + \frac{1 - 2\chi}{2}\rho + \frac{\rho^2}{6} + \text{higher order terms.} \tag{2.54}$$

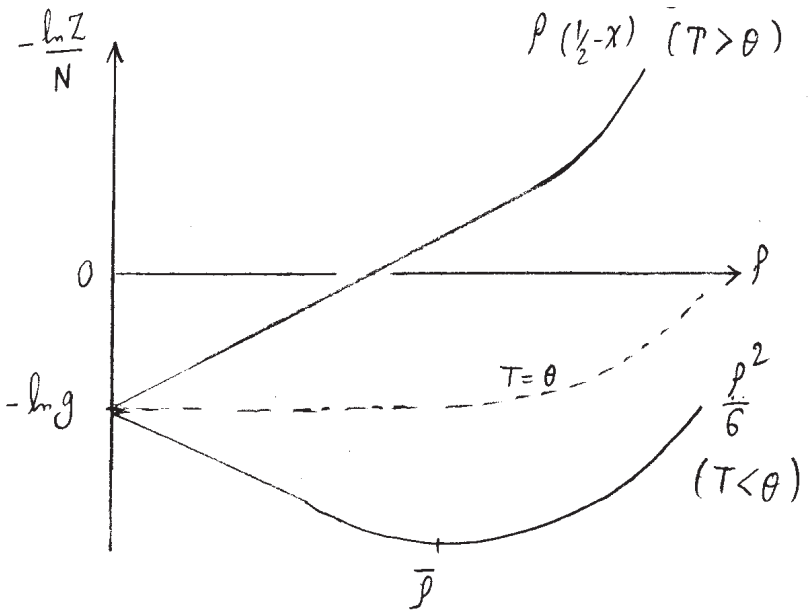

Figure 8: Variational free energy for a compact polymer.

The optimal density for $T < \theta$ is obtained by minimizing the above free energy,

$$-\frac{1}{N}\frac{d\ln Z}{d\rho} = \left(\frac{1}{2} - \chi\right) + \frac{\rho}{3} + \cdots,$$

leading to

$$\overline{\rho} = 3\left(\chi - \frac{1}{2}\right) + \cdots, \tag{2.55}$$

i.e. a density that vanishes linearly on approaching the θ-temperature from below. The higher order terms ensure that the density does not exceed the maximum value of unity in a fully compact state.

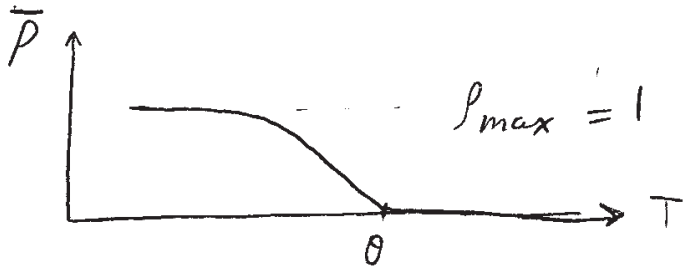

Figure 9: Variation of density in a compact polymer.

From Eq. (2.48) we note that the energy gain per particle from the attractive interactions

satisfies

$$\frac{E_{att.}}{N} = -\overline{\rho}\chi k_B T\,. \tag{2.56}$$

The entropy per particle is then given by

$$\frac{S}{Nk_B} = \frac{-F+E}{Nk_BT} = \frac{\ln Z}{N} - \overline{\rho}\chi = \ln g + \frac{3}{2}\left(\chi - \frac{1}{2}\right)^2 + \cdots - \overline{\rho}\chi \approx \ln g - \frac{\overline{\rho}}{2} + \mathcal{O}(\overline{\rho}^2)\,. \tag{2.57}$$

(The final expression includes only the leading linear term as $\chi \to 1/2$.) Thus close to the θ-temperature the entropy is reduced, initially linearly in temperature, although it also will eventually saturate as does the density. The above analysis is reminiscent of the mean-field analysis of the transition between a gas (low density) and a liquid (high density). The liquid state still encompasses many particle configurations, although fewer than in a gas. Further cooling of liquids typically leads to frozen states with even lower entropy. We may thus inquire if such a freezing transition also exists for polymers.

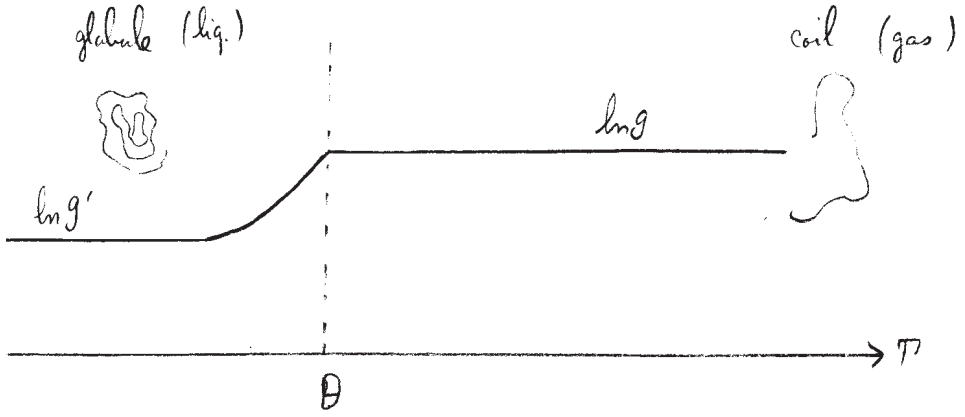

Figure 10: Variation of entropy in a compact polymer.